

PFC/JA-96-50

## Impurity Transport in Alcator C-Mod Plasmas

J.E. Rice, J.L. Terry, J.A. Goetz, Y. Wang,  
E.S. Marmor, M. Greenwald, I.H. Hutchinson,  
Y. Takase, S. Wolfe, H. Ohkawa, A. Hubbard

November 1996

Submitted to Physics of Plasmas.

This work was supported by the U. S. Department of Energy Contract No. DE-AC02-78ET51013. Reproduction, translation, publication, use and disposal, in whole or in part by or for the United States government is permitted.

## Impurity transport in Alcator C-Mod plasmas

J. E. Rice, J. L. Terry, J. A. Goetz, Y. Wang, E. S. Marmor,  
M. Greenwald, I. Hutchinson, Y. Takase, S. Wolfe, H. Ohkawa, A. Hubbard  
*Plasma Fusion Center, Massachusetts Institute of Technology*  
*175 Albany St.*  
*Cambridge, MA 02139-4307*

### Abstract

Trace non-recycling impurities have been injected into Alcator C-Mod [I. H. Hutchinson et al., Phys. Plasmas 1 (1994) 1511.] plasmas in order to determine impurity transport coefficients. Subsequent impurity emission has been observed with spatially scanning x-ray and Vacuum Ultra-Violet (VUV) spectrometer systems. Measured time-resolved brightness profiles of helium- and lithiumlike transitions have been compared with those calculated from a transport code which includes impurity diffusion and convection in conjunction with an atomic physics package for individual line emission. During L-mode plasmas, the transport can be characterized by pure diffusion, with coefficients  $\sim 5000 \text{ cm}^2/\text{sec}$ , reflecting the  $\sim 20$  ms decay in the x-ray and VUV line brightnesses. During H-modes, the impurity confinement times are much longer, and the modelling requires that there be a strong inward convection (of order  $1000 \text{ cm}/\text{sec}$ ) near the plasma edge, with greatly reduced diffusion (of order  $100 \text{ cm}^2/\text{sec}$ ), also in the region of the edge transport barrier. These edge values of the transport coefficients during H-mode are qualitatively similar to the neo-classical values. Nitrogen has also been injected, and after the H- to L-mode transition, the inner shell satellite lines of lithiumlike nitrogen dominate in intensity the resonance line of heliumlike  $\text{N}^{5+}$  in a thin shell near the plasma edge.

PACS: 52.25.Fi, 52.25.Vy, 52.25.Nr, 52.25.Q

## I. Introduction

Impurities can play an crucial role in fusion plasma performance through radiation losses and dilution of fuel in the plasma core [1,2]. It is therefore important to understand the impurity sources and subsequent transport into the plasma [3]. The employment of injected non-intrinsic, non-recycling impurities allows for the isolation and study of impurity transport [4]. In L-mode plasmas, the impurity confinement is generally found to be short [5-9], and intrinsic impurity radiation is not a dominant player in the overall energy balance. However, in enhanced energy confinement H-mode plasmas, impurity confinement can be very long [10-13] and play an important role in the energy balance. In the case of Alcator C-Mod [14], with power densities in the range of fusion reactors, it is of interest to characterize impurity transport in a reactor-relevant setting.

For Alcator C-Mod, the impurity transport coefficient profiles have been determined for L-, ELMy H- and ELM-free H-mode plasmas. In Sec. II the impurity injection experiments are described. In Sec. III the determination of the impurity transport coefficient profiles are presented, in addition to the first observations of the inner shell satellites in lithiumlike nitrogen.

## II. Experiment Description

The measurements described here were performed on the Alcator C-Mod tokamak [14], a compact ( $a = 22.5$  cm,  $R = 67$  cm), diverted (with  $\kappa \leq 1.8$ ), high field ( $B_T \leq 8$  T) device with molybdenum plasma facing components. Scandium has been injected into L- and H-mode plasmas using the laser blow-off technique [4]. Nitrogen has been puffed through a piezo-electric valve. Scandium x-ray emission was recorded by a spatially scanable x-ray spectrometer array [15], each spectrometer of which has a resolving power of 5000, a 2 cm spatial resolution and a luminosity function of  $7 \times 10^{-9}$  cm<sup>2</sup>-sr, with spectra typically collected every 20 ms. In most of the analysis presented here, the resonance line ( $1s2p \ ^1P_1 - 1s^2 \ ^1S_0$ ) of heliumlike

Sc<sup>19+</sup> at 2.8731 Å [16,17] has been used. For the VUV emission, an absolute-intensity-calibrated spatially scanning VUV spectrograph [18] has been employed to monitor the brightness of the 1s<sup>2</sup>2s - 1s<sup>2</sup>2p transition in lithiumlike Sc<sup>18+</sup> at 279.8 Å, and heliumlike N<sup>5+</sup> resonance, intercombination and inner shell satellite lines around 28 Å (in third order). This spectrometer has ~0.6 Å 1<sup>st</sup> order spectral resolution and 2 cm spatial resolution, with spectra collected typically every 4 - 16 ms. Both spectrometer systems can view all of the plasma, out to the last closed flux surface.

The impurity transport coefficients D(r) and V(r) have been determined from the time evolution of the radial brightness profiles of the helium- and lithiumlike x-ray and VUV transitions of injected impurities. The spatial variations, time histories and relative intensities of these profiles place a very strong constraint on the selection of the transport coefficient profiles.

### III. Determination of the Impurity Transport Coefficients

For the case of L-mode plasmas, the impurity confinement times are short, nominally around 20 ms. A typical example of the time histories of central chord helium- (dots) and lithiumlike (asterisks) scandium brightnesses is shown in Fig.1. The radiation from the two charge states (the x-ray signal has been increased by a factor of 100 for easier direct comparison) peaks sequentially in time, and the scandium has totally left the plasma within 100 ms after the injection. For this particular discharge, at the time of injection (.75 s), the plasma current was 1.2 MA, the toroidal magnetic field was 7.9 T, the central electron density was  $2.0 \times 10^{14}/\text{cm}^3$ , the central electron temperature was 2800 eV, and there were 1.0 MW of auxilliary ICRF heating power. For most Alcator C-Mod electron temperature profiles, heliumlike scandium is a central charge state, while lithiumlike radiates mostly from the outer third of the plasma. Also shown in the figure by the curves are the simulated central chord brightness time histories. In these calculations, the

impurity charge state densities were taken from the Multiple Ionization State Transport (MIST) code [19], the electron density and temperature profiles were measured from a two color laser interferometer [20] and an electron cyclotron emission interferometer [21], the line emission was calculated a la Ref.[22], and the brightness line integrals were performed through the appropriate flux surfaces [23]. Not only is the agreement between the time histories of the measured and calculated lines quite good, but the relative intensities of the simulated and observed lines are also excellent. Here, there is only one normalization used (of the VUV line), which determines the scandium density in the plasma at one time. This agreement is taken to validate the use of the L-mode transport coefficients, which are shown in Fig.2 by the solid lines. The diffusion coefficient is  $5000 \text{ cm}^2/\text{sec}$  over most of the plasma interior, and then drops to about  $500 \text{ cm}^2/\text{sec}$  near the last closed flux surface; there is no need for any convection velocity in this simulation, similar to what was found in Alcator A and C [5,7]. Inclusion of any inward convection velocity would cause the predicted Li-like scandium signal to increase much more quickly than is observed; effects on the predicted He-like signal in this case would be insignificant. Shown for comparison in Fig.2 are calculated neo-classical transport coefficients [24] (dotted lines), which are qualitatively and quantitatively different, and in the case of L-mode plasmas, the impurity transport may be regarded as anomalous [5-8].

In ELMy H-mode plasmas, the impurity confinement times are considerably longer, of order of a few hundred milliseconds. For the case of 0.8 MA, 5.3 T, H-mode plasmas with 2.5 MW of ICRF power, a central electron density of  $3.7 \times 10^{14}/\text{cm}^3$  and central electron temperature of 3200 eV, the time evolution of the scandium x-ray and VUV spatial brightness profiles at various times after the injection are shown in Figs. 3 and 4, respectively. The central x-ray brightness gradually reaches a zenith about 100 ms after the injection, in contrast to the L-mode case where the intensity peaked after about 20 ms. The maximum brightness is a factor of 3 higher in the H-mode case. Shown by the smooth curves in the figure are the simulations, which are in good agreement. In the VUV case (Fig.4), the signal levels are also higher by a factor of 3 compared to L-mode, and the

decay times are much longer. (The same amount of scandium as in the L-mode case was injected.) The central chord brightness peaks in about 30 ms (as does the whole profile), and the overall profile has only slightly decayed by 150 ms after the injection. Again, the simulations, shown by the smooth curves, are in good agreement with the data. The transport coefficient profiles for these calculations are also shown in Fig.2. In the ELMy H-mode case, the diffusion coefficient in the center is slightly reduced compared to L-mode, and greatly reduced in the outer third of the plasma, where it is close to the neo-classical value. In this case it is also necessary to include inward convection at the edge, of magnitude -700 cm/sec. This shape is qualitatively like the neo-classical profile. The indication is that in H-mode plasmas, whatever mechanism(s) is (are) responsible for the anomalous impurity transport is (are) suppressed in the vicinity of the edge transport barrier [25], and the transport becomes more like neo-classical. Similar conclusions about the large (factor of 10) drop in the edge diffusion coefficient, along with the large increase in the inward convection velocity at the edge, in going from L-mode to H-mode plasmas were reached in the case of JET[13]. However, the magnitudes of the *central* diffusion coefficients in JET are much lower than in Alcator C-Mod.

For the case of ELM-free H-mode, the impurity confinement times are even longer than in ELMy H-mode plasmas, and the transport is so slow that the impurity signals don't reach a peak during the ELM-free period, as demonstrated in Fig.5. The ELM-free period begins at .6 sec shortly after the ICRF power was turned on, and the scandium was injected at .7 sec. The  $\text{Sc}^{18+}$  brightness increases steadily following the injection, and begins to decay at .86 sec when the ELM-free period ends, as seen on the  $D_\alpha$  signal. The total radiated power also increases steadily during this time, until the radiation dominates the input power, causing the stored energy to drop. During the subsequent 'enhanced  $D_\alpha$  H-mode' [25,26] (.86 - 1.04 s), the impurity confinement time is reduced to  $\sim 100$  ms, as reflected in the decay of the scandium signal, and the radiated power decreases as well, allowing the stored energy to rise again. The ICRF heating power turns off at 1.04 sec, and the plasma reenters L-mode at 1.135 sec, when the scandium decays with a confinement time

of around 20 ms, the nominal L-mode value. The scandium has remained in the plasma for 500 ms. During the ELM-free period, the impurity transport coefficient profiles are qualitatively similar to those in the ELMMy case, but quantitatively, the diffusion coefficient drops to an even lower value ( $\sim 50 \text{ cm}^2/\text{sec}$ ) near the transport barrier at the edge, where the convection velocity reaches a more negative value ( $-3000 \text{ cm}/\text{sec}$ ), as shown in Fig.2. Such a low value for the diffusion leads to very long impurity confinement ( $> 1 \text{ sec}$ ) and this is why the VUV signal in Fig.5 is unable to reach a peak and begin to decay before the plasma goes out of ELM-free H-mode. The coefficients in the enhanced  $D_\alpha$  H-mode are similar to those in the ELMMy case.

#### IV. Inner Shell Satellites of Nitrogen

There are some interesting and subtle manifestations of the edge transport coefficient profiles in the intensities of impurity emission from the plasma periphery. The slow *edge* impurity transport of L-mode enables the inner shell satellites of lithiumlike nitrogen to dominate the the resonance line of heliumlike  $\text{N}^{5+}$  in the extreme edge of the plasma. For most Alcator C-Mod operating conditions for viewing chords out to  $r/a = 0.8$ , the  $\text{N}^{5+}$  spectrum near  $29 \text{ \AA}$  is comprised of only two lines, the resonance line, w ( $1s2p \ ^1P_1 - 1s^2 \ ^1S_0$  at  $28.787 \text{ \AA}$ ) and the intercombination line, y ( $1s2p \ ^3P_1 - 1s^2 \ ^1S_0$  at  $29.084 \text{ \AA}$ ). At the extreme plasma periphery ( $r/a \geq 0.9$ ), the inner shell satellites [16] q ( $1s2s2p \ ^2P_{3/2} - 1s^2 2s \ ^2S_{1/2}$  at  $29.441 \text{ \AA}$ ), r ( $1s2s2p \ ^2P_{1/2} - 1s^2 2s \ ^2S_{1/2}$  at  $29.443 \text{ \AA}$ ), s ( $1s2s2p \ ^2P_{3/2} - 1s^2 2s \ ^2S_{1/2}$  at  $29.155 \text{ \AA}$ ) and t ( $1s2s2p \ ^2P_{1/2} - 1s^2 2s \ ^2S_{1/2}$  at  $29.155 \text{ \AA}$ ) are also visible, as seen in Fig.6. The lines y, s and t form an unresolved composite at  $29.1 \text{ \AA}$  and q and r comprise an unresolved feature at  $29.5 \text{ \AA}$ . In the top frame of Fig.6 is a spectrum obtained along a viewing chord at  $20.5 \text{ cm}$  ( $r/a = .91$ ) during the ELMMy period of a  $5.3 \text{ T}$  discharge with nitrogen injection, and the resonance line still dominates the spectrum. In the bottom frame of the figure is a spectrum obtained from the same viewing chord after the same plasma has reentered L-mode, and the satellites q and

r have become the strongest lines. Also shown in the figure by the smooth curves are synthetic spectra whose line intensities are generated from calculated brightness profiles and whose wavelengths are taken from Ref.[16]. The relative intensities of the calculated lines are in good agreement with the observations, while there is a slight shift (.35 Å) between the measured and calculated wavelengths for q and r. The brightnesses were determined from the calculated emissivity for the six lines, which are shown in Fig.7. In the top frame are the profiles near the edge generated using the the ELMy transport coefficients of Fig.2, and in the bottom frame are shown the profiles for the L-mode case. Shown by the thin lines are the helium- and lithiumlike density profiles. In both cases the satellite lines are emitted in a thin shell around 20.5 cm, in spite of the fact that the H- and L-mode electron temperature profiles are different. In the L-mode case the satellites are the dominant lines at 20.5 cm because there is no inward convection to sweep the lithiumlike nitrogen quickly through the region where the electron temperature is appropriate for the excitation of these lines, before ionization occurs.

## V. Conclusions

Profiles for the impurity transport coefficients have been determined by analyzing the line emission from injected impurities in Alcator C-Mod L-mode, ELMy H-mode and ELM-free plasmas. The brightness time histories and relative intensities of He- and Li-like scandium, following injection into L-mode plasmas, are well described by an anomalously large diffusion coefficient ( $\sim 5000 \text{ cm}^2/\text{sec}$ ) over most of the plasma volume, which falls to  $\sim 500 \text{ cm}^2/\text{sec}$  near the edge. In L-mode, there is no necessity for the inclusion of any inward convection, and impurity confinement times are  $\sim 20 \text{ ms}$ . In the case of ELMy H-mode plasmas the impurity confinement times are much longer (hundreds of milliseconds), and analysis of the scandium x-ray and VUV brightness profile time histories after injection reveals a large reduction in the diffusion coefficient (to  $\sim 500 \text{ cm}^2/\text{sec}$ ) in the outer 1/4 of the plasma, coupled with the appearance of a large ( $-700 \text{ cm/s}$ ) inward convection



velocity near the last closed flux surface. For ELM-free discharges the impurity confinement is very long (several seconds), so long that the accumulation of intrinsic impurities leads to total radiated power in excess of the input power, which in turn causes the ELM-free period to end on a time scale much shorter than the impurity confinement time. Modelling of the x-ray and VUV brightness profiles suggests that the diffusion coefficient at the edge is  $\sim 50 \text{ cm}^2/\text{sec}$ , with an inward convection velocity of  $-3000 \text{ cm}/\text{sec}$ . It is interesting to note that in going from L-mode to ELMy H-mode to ELM-free H-mode, the energy confinement time also correspondingly increases [10,25].

The values of the transport coefficients near the plasma edge have some interesting repercussions on the relative intensities of lines in the heliumlike nitrogen spectrum. The slow diffusion (with no inward convection) at the edge during L-mode plasmas allows inner shell excitation of lithiumlike nitrogen, which occurs in a thin layer just inside the last closed flux surface, to dominate excitation of the heliumlike resonance line.

### **Acknowledgements**

The authors would like to thank J. Irby for electron density measurements, P. O'Shea for electron temperature measurements and the Alcator C-Mod operations group for expert running of the tokamak. Work supported at the Massachusetts Institute of Technology by United States Department of Energy Contract No. DE-AC02-78ET51013.

## References

- [1] J. Wesson, Tokamaks, Oxford University Press, Oxford (1987).
- [2] M. Shimada, Fusion Engineering and Design **15** (1992) 325.
- [3] J.E.Rice, E.S.Marmar, B.Lipschultz and J.L.Terry, Nucl. Fusion **24** (1984) 329.
- [4] E. Marmar, J. Cecchi and S. Cohen, Rev. Sci. Instrum. **46** (1975) 1149.
- [5] E. S. Marmar, J. E. Rice and S. L. Allen, Phys Rev. Lett. **45** (1980) 2025.
- [6] TFR Group, Phys. Lett. **87A** (1982) 169.
- [7] E. S. Marmar, J. E. Rice, J. L. Terry and F. Seguin, Nucl. Fusion **22** (1982) 1567.
- [8] TFR Group, Nucl. Fusion **23** (1983) 559.
- [9] B.C. Stratton, A.T. Ramsey, F.P. Boody et al., Nucl. Fusion **27** (1987) 1147.
- [10] G. Fussman, J. Hofmann, G. Janeschitz et al., J. Nucl. Mater. **162** (1989) 14.
- [11] K. Ida, R.J. Fonck, S. Sesnic, R.A. Hulse, B. LeBlanc and S.F. Paul, Nucl. Fusion **29** (1989) 231.
- [12] M.E. Perry, N.H.Brooks, D.A.Content, R.A.Hulse, M.A. Mahdavi and H.W.Moos, Nucl. Fusion **31** (1991) 1859.
- [13] D. Pasini, R.Giannella, L.L.Taroni, M.Mattioli, B.Denne-Hinnov, N.Hawkes, G.Magyar and H.Weisen, Plasma Physics and Controlled Fusion **34** (1992) 677.
- [14] I.H.Hutchinson, R.Boivin, F.Bombarda, P.Bonoli, S.Fairfax, C.Fiore, J.Goetz, S.Golovato, R.Granetz, M.Greenwald, S.Horne, A.Hubbard, J.Irby, B.LaBombard, B.Lipschultz, E.Marmar, G.McCracken, M.Porkolab, J.Rice, J.Snipes, Y.Takase, J.Terry, S.Wolfe, C.Christensen, D.Garnier, M. Graf, T. Hsu, T. Luke, M. May, A.Niemczewski, G.Tinios, J.Schachter and J.Urbahn, Phys. Plasmas **1** (1994) 1511.
- [15] J.E.Rice and E.S.Marmar, Rev. Sci. Instrum. **61** (1990) 2753.
- [16] L. A. Vainshtein and U. I. Safronova, Atomic Data and Nuclear Data Tables **21**, (1978) 49.
- [17] J.E.Rice, M.A.Graf, J.L.Terry, E.S.Marmar, K.Giesing and F.Bombarda, J. Phys. B **28** (1995) 893.
- [18] M.A. Graf, J.E. Rice, J.L. Terry, E.S. Marmar, J.A. Goetz, G.M. McCracken,

- F. Bombarda and M.J. May, *Rev. Sci. Instrum.* **66** (1995) 636.
- [19] R. A. Hulse, *Nucl. Tech./Fus.* **3** (1983) 259.
- [20] J.H.Irby, E.S. Marmor, E. Sevillano and S.M. Wolfe, *Rev. Sci. Instrum.* **59** (1988) 1568.
- [21] T.C.Hsu, A. Hubbard and I.H. Hutchinson, *Proc. 8th Joint Workshop on ECE and ECRH, IPP III/186* (1993) 409.
- [22] R.Mewe, *Astron. and Astrophys.* **20** (1972) 215.
- [23] L. L. Lao, H. St.John, R.D. Stambaugh, A.G. Kellman and W. Pfeiffer, *Nucl. Fusion* **25** (1985) 1611.
- [24] R. Hawryluk, S. Suckewer and S. Hirshman, *Nucl. Fusion* **19** (1979) 607.
- [25] M. Greenwald, R.L. Boivin, F. Bombarda, P. Bonoli, C. Fiore, D. Garnier, J. Goetz, S. Golovato, M. Graf, R. Granetz, S. Horne, A. Hubbard, I. Hutchinson, J. Irby, B. LaBombard, B. Lipschultz, E. Marmor, M. May, G. McCracken, P. O'Shea, J. Rice, J. Schachter, J. Snipes, P. Stek, Y. Takase, J. Terry, Y. Wang, R. Watterson, B. Welch, S. Wolfe, 'H Mode Confinement in Alcator C-Mod', submitted to *Nucl. Fusion* (1996) .
- [26] Y. Takase, B. Boivin, F. Bombarda, P. Bonoli, C. Fiore, D.Garnier, J. Goetz, S. Golovato, R. Granetz, M. Greenwald, S. Horne, A. Hubbard, I. Hutchinson, J. Irby, B. LaBombard, B. Lipschultz, E. Marmor, M. May, A. Mazurenko, G. McCracken, P. O'Shea, M. Porkolab, J. Reardon, J. Rice, C. Rost, J. Schachter, J. Snipes, P. Stek, J. Terry, R. Watterson, B. Welch, S. Wolfe, "High Power Density H-Modes in Alcator C-Mod," *Proceedings of the 16th IAEA Fusion Energy Conference, Montreal, 1996* (to be published, IAEA, Vienna, 1997), paper F1-CN-64/A5-4.

## Figure Captions

Fig.1 The observed brightness time histories for lithiumlike (asterisks) and heliumlike (dots) line emission for a scandium injection at .75 s into an L-mode plasma, and the simulations (smooth curves). The x-ray data and simulation have been increased by a factor of 100 for direct comparison with the VUV traces. (1 GR =  $10^{15}$  photons/cm<sup>2</sup>/sec.)

Fig.2 Impurity transport coefficient profiles, with the diffusion coefficients shown in the top and the convection velocities shown in the bottom. The solid curves are for L-mode plasmas, dashed for ELMy H-modes, dash-dot-dash for ELM-free H-modes, and dotted for the calculated neo-classical values.

Fig.3 ELMy H-mode x-ray brightness profiles at three times after the injection (symbols), and the simulations (curves).

Fig.4 ELMy H-mode VUV brightness profiles at three times after the injection (symbols) and the simulations (curves).

Fig.5 Time histories of some parameters of interest for an ELM-free H-mode plasma. From top to bottom are shown the Sc<sup>18+</sup> signal, the D<sub>α</sub> brightness, the total radiated power, the plasma stored energy and the input ICRF power.

Fig.6 Heliumlike nitrogen spectra including inner shell satellite lines during the ELMy H-mode (top) and L-mode (bottom) phase of a plasma with nitrogen injection, obtained from a chord viewing the edge plasma at 20.5 cm (r/a = .91). Shown by the smooth curves are synthetic spectra.

Fig.7 Calculated nitrogen emissivity profiles for H-mode (top) and L-mode (bottom) plasmas. The resonance and intercombination lines (w and y) of heliumlike nitrogen are solid, and the inner shell lithiumlike lines (q, r, s and t) are shown as

dash-dot-dot-dot-dash lines. The heliumlike and lithiumlike *densities* (same scale but in units of  $\text{cm}^{-3}$ ) are shown by the thin lines.

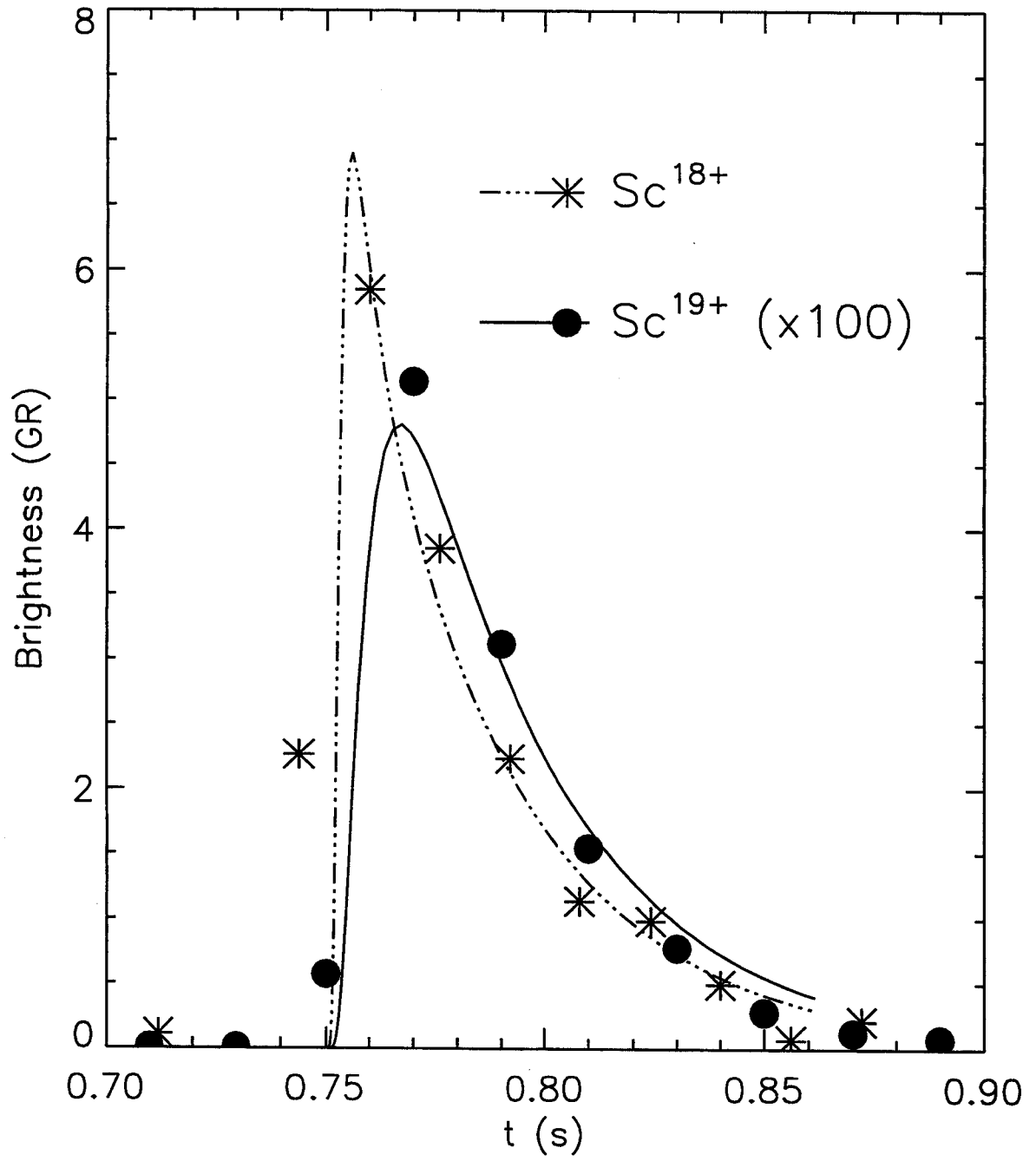


Figure 1

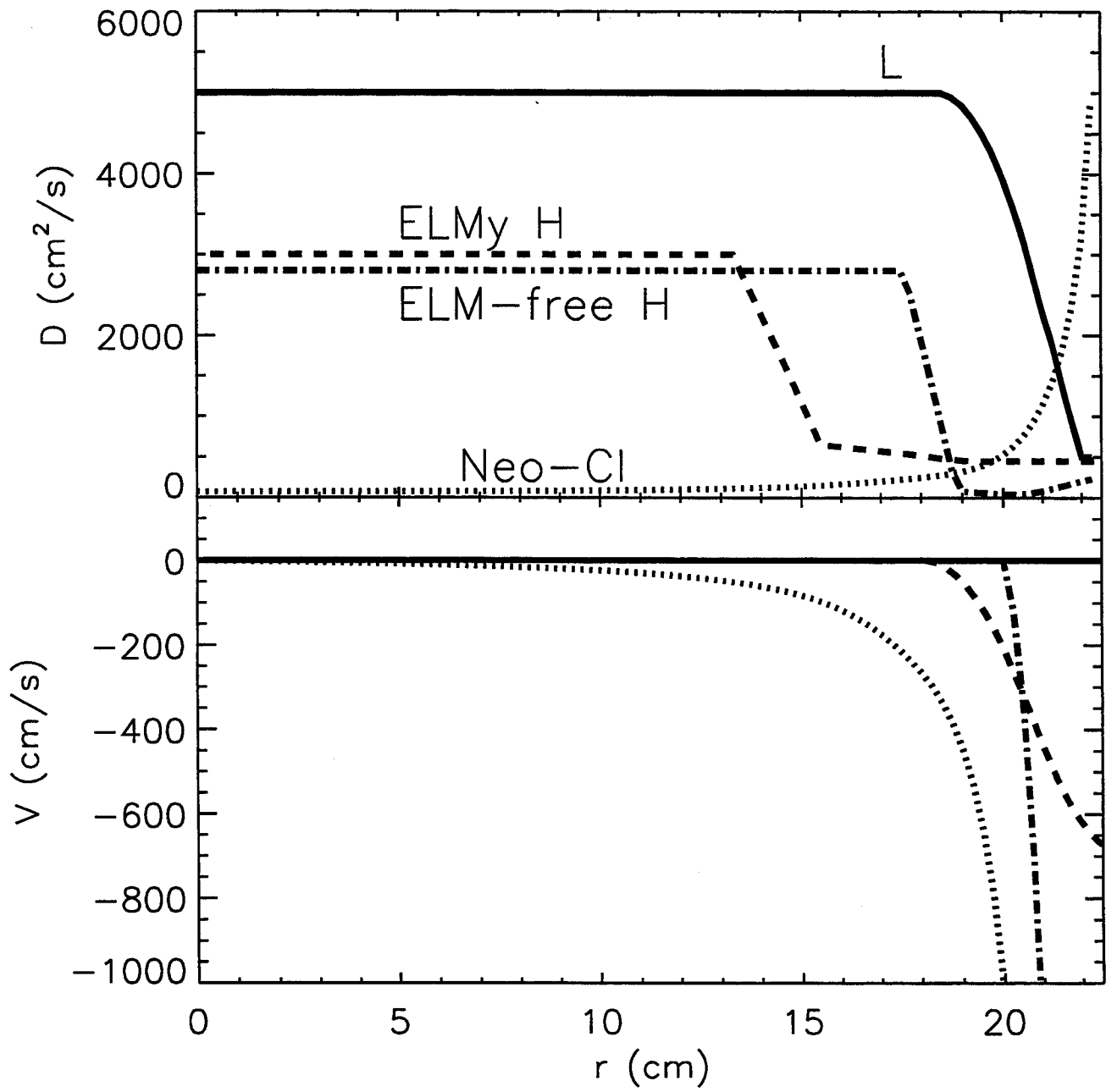


Figure 2

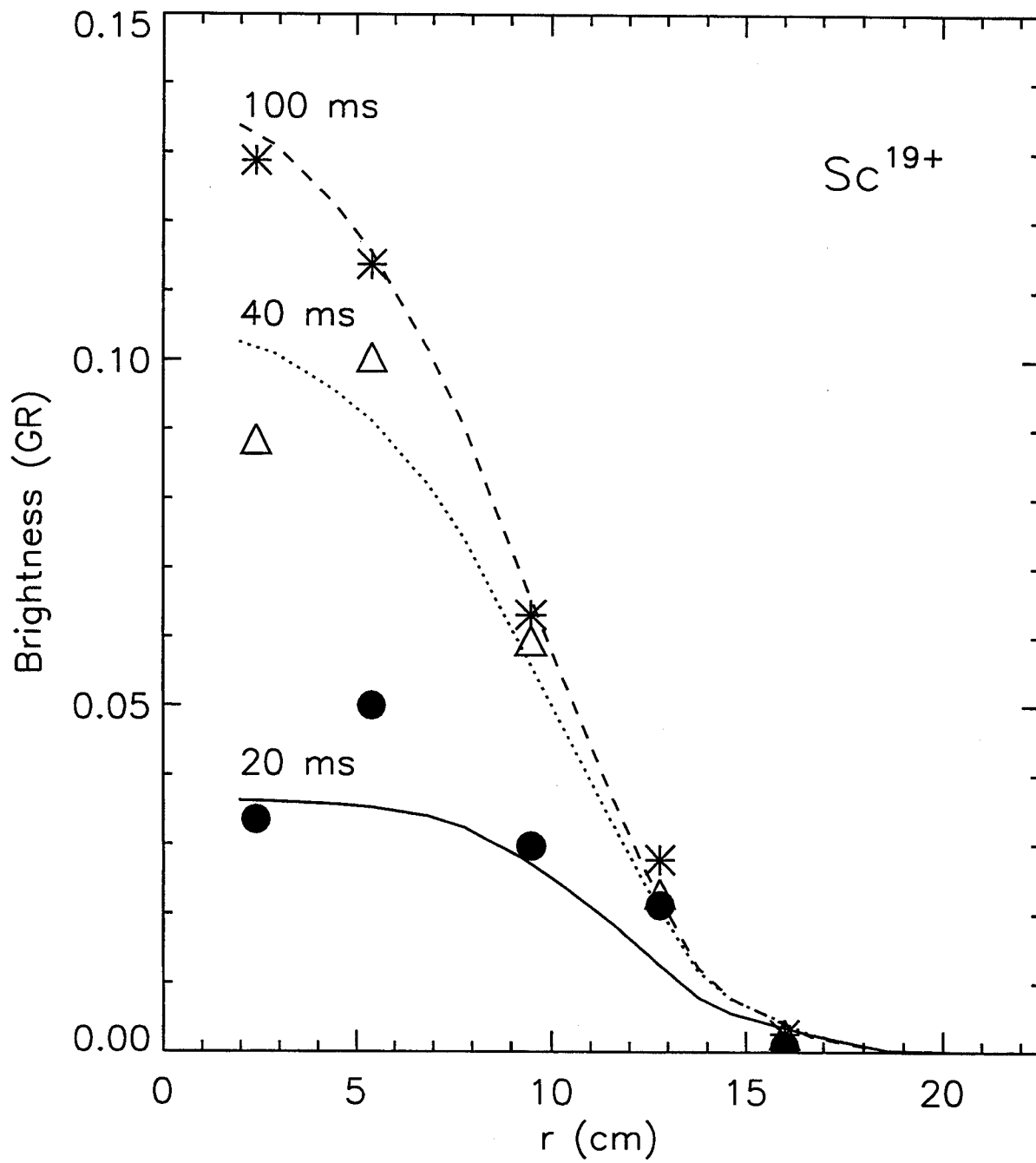


Figure 3



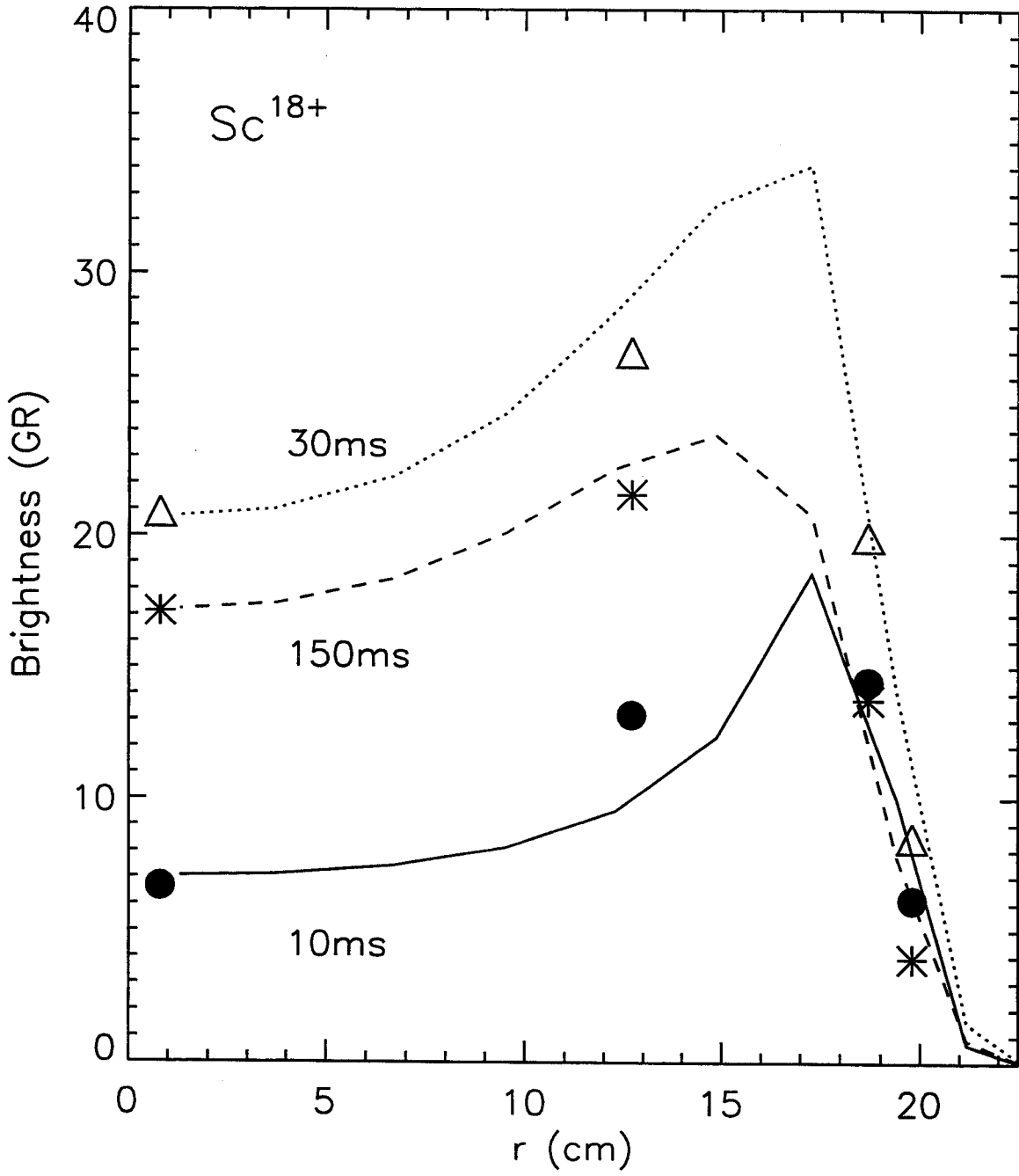


Figure 4

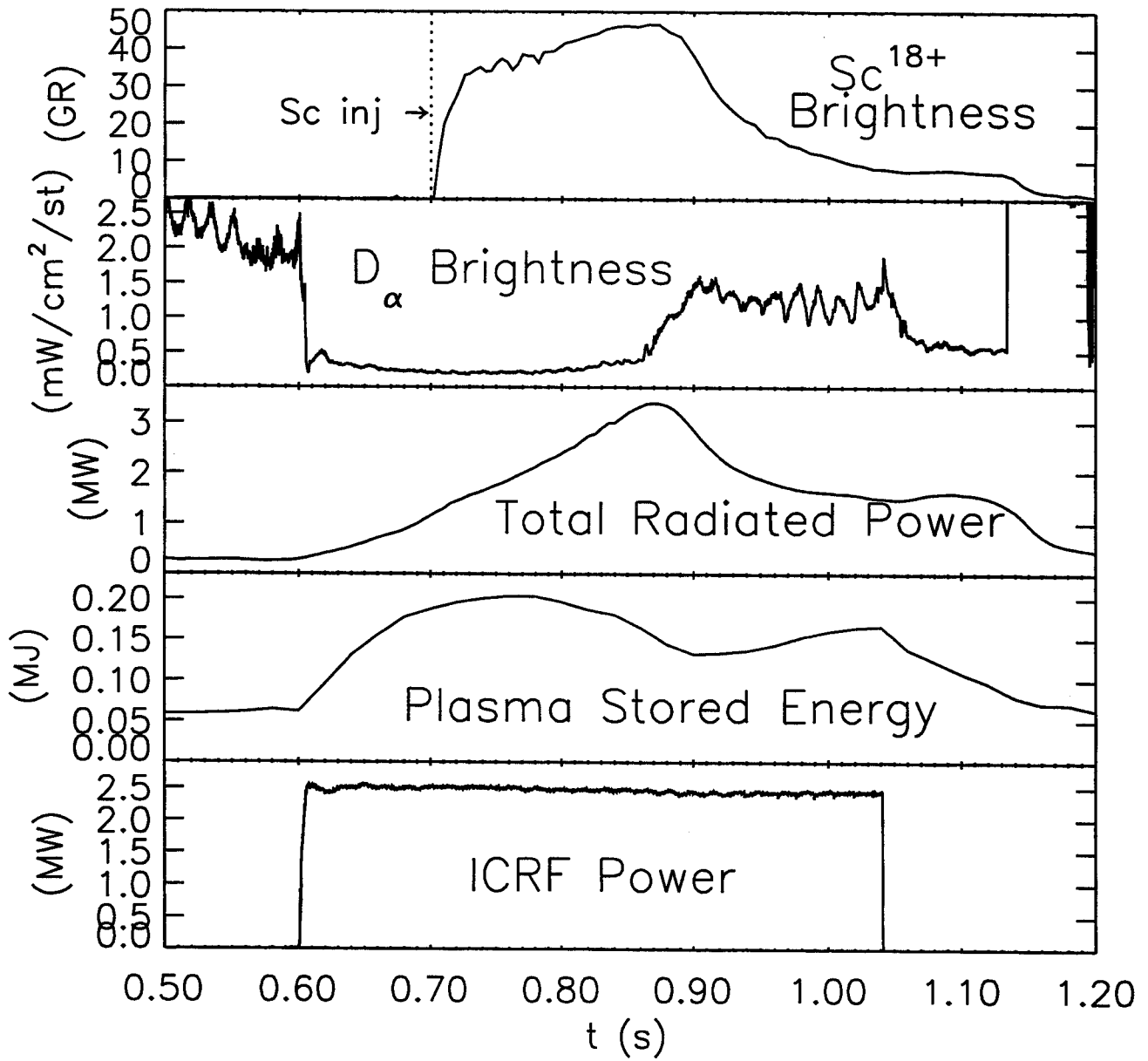


Figure 5

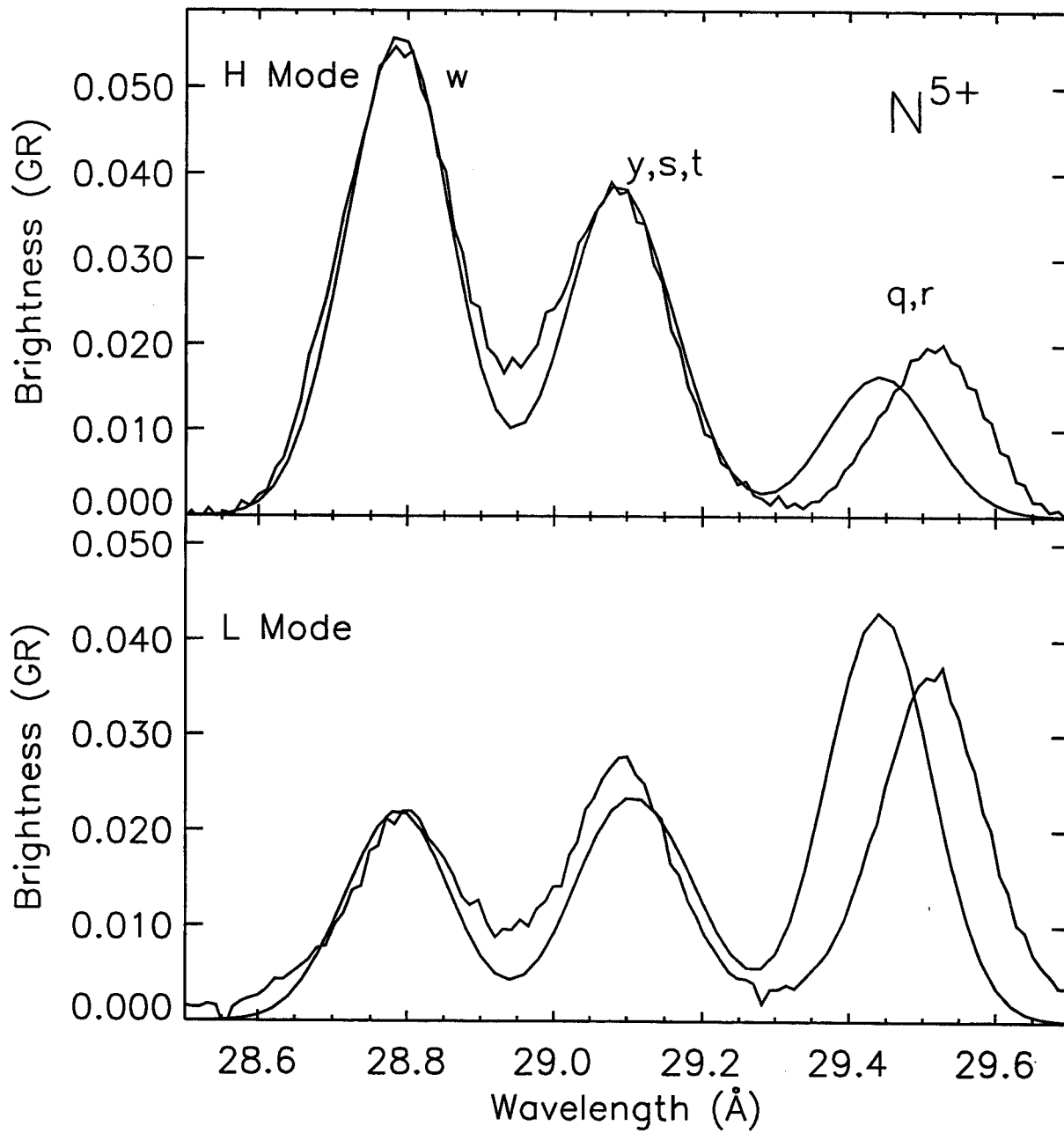


Figure 6

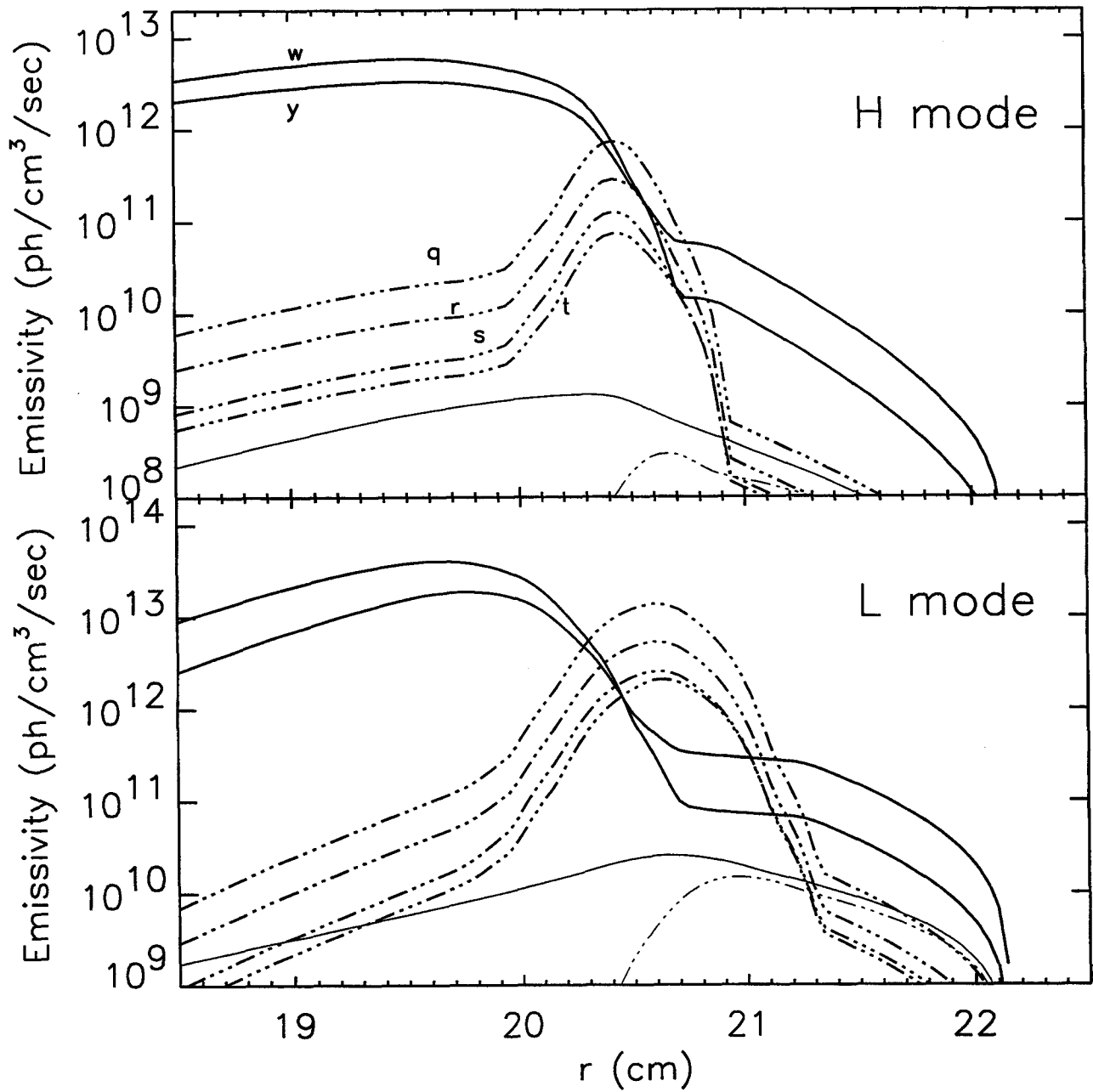


Figure 7